



## Archeometric study of pottery shards from Conjunto Vilas and São João, Amazon

L.S.S. Oliveira<sup>a</sup>, C.M. Abreu<sup>a</sup>, F.C.L. Ferreira<sup>b</sup>, R.C.A. Lopes<sup>c</sup>, F.O. Almeida<sup>c</sup>, E.K. Tamanaha<sup>d</sup>, J.S. Belletti<sup>d</sup>, R. Machado<sup>a</sup>, M.A. Rizzutto<sup>e</sup>, D.N. Souza<sup>a,\*</sup>

<sup>a</sup> Department of Physics, Federal University of Sergipe, São Cristóvão, SE, Brazil

<sup>b</sup> Department of Physics, Federal University Sul e Sudeste do Pará, Marabá, PA, Brazil

<sup>c</sup> Department of Archeology, Federal University of Sergipe, Laranjeiras, SE, Brazil

<sup>d</sup> Instituto de Desenvolvimento Sustentável Mamirauá, IDS-M-OS, Tefé, AM, Brazil

<sup>e</sup> Institute of Physics, University of São Paulo, São Paulo, SP, Brazil

### ARTICLE INFO

#### Keywords:

Ancient pottery  
Archeometry  
Brazilian amazon  
Pocó-Tefé-Caiambé occupation phases

### ABSTRACT

In this work, we investigated through archeometry studies the mineralogical composition of pottery shards from Conjunto Vilas and São João archeological sites located in the macro-region of middle Solimões, in the State of Amazonas, Brazil. Archeometric analyses are fundamental for classification and characterization of ancient ceramics, providing relevant data that can furnish information about production processes, types of use and social meaning of these materials. The shards were studied by optical microscopy (OM), Fourier transform infrared (FTIR) spectroscopy, energy dispersive x-ray fluorescence (ED-XRF), X-ray diffraction (XRD), and scanning electron microscopy, coupled with energy-dispersive X-ray analysis (SEM-EDX). Al, Si, K, Ca, Ti and Fe (as oxides) were identified among other minority elements in the ceramic pastes, besides the presence of cauxi and caraipé (non-plastic materials), as well as possibly shells. The crystalline phases identified were quartz, hematite, kaolinite, anatase, dolomite and illite-muscovite, being that the kaolinite was found more frequently in ceramics. The results obtained in this work add important information about the analyzed artifacts, allowing a better understanding of the ancient civilizations from the Amazon region.

### 1. Introduction

In the last decades, the Brazilian Amazon has been the scene of important archeological discoveries which serve as a basis for possible explanations about ancient human civilizations in that region. Among the numerous discoveries of archeological sites currently cataloged in the Amazon region, those that have anthrosols (Archeological Dark Earth – ADE) stand out (Garcia et al., 2015). This type of soil is called “Indian black earth” by natives (Terra Preta de Índio in Portuguese), and constitutes archeological evidence of ancient human settlements (Costa et al., 2004). The sites named Conjunto Vilas and São João, located in the middle Solimões River, in the Tefé municipality, State of Amazonas, Brazil, are examples of sites where such anthrosols are found (Belletti, 2015; Lopes, 2018).

Peter Hilbert was one of the first archeologists to study systematically the region of the middle Solimões River (Hilbert, 2009). One of Hilbert's works was on the definition of archeological material of that region in two chronological and/or spatial occupation phases, named

Caiambé and Tefé, which are also names of lakes of that region. Ceramic phases have been defined based on the decoration and form of the pottery, and mostly on the type of non-plastic clay added to raw clay during its production (Hazenfratz et al., 2016). Other archeologists have explored the region. In one recent study, Belletti (2015) carried out effected excavations and analyses at Conjunto Vilas, which had been first recorded in 1955, and found artifacts with characteristics of the Pocó phase. In another study, Lopes (2018) investigated the São João site, which is about 35 km from Conjunto Vilas. For both researchers, the object of study was painted ceramic (shards) from Tefé and Caiambé phases. The Pocó phase occupation dated from 100 B.C. (Silverman, 2008) until the middle of the first millennium of the Christian era (A.D.), the Caiambé phase occupation extended from 100 to 800 A.D., and the Tefé phase between 900 and 1300 A.D. (Hilbert and Hilbert, 1980).

The use of techniques drawn from physics, chemistry, biology, museology and anthropology is necessary for detailed characterizations of the historical-cultural aspects of ancient materials. Such a

\* Corresponding author.

E-mail address: [divanizi@ufs.br](mailto:divanizi@ufs.br) (D.N. Souza).

<https://doi.org/10.1016/j.radphyschem.2019.04.053>

Received 14 December 2018; Received in revised form 23 April 2019; Accepted 25 April 2019

Available online 04 May 2019

0969-806X/ © 2019 Elsevier Ltd. All rights reserved.



Fig. 1. Location of Conjunto Vilas and São João sites. Source: Google Earth (accessed 03/29/2018). Map of Brazil with the Amazonas region shown (UTM 20M 0313990 9628446/20M 0341007 9611394).

multidisciplinary approach can add relevant information to archaeological studies, and is known as archeometry (Artioli, 2010).

In this work we used imaging and spectroscopic analytical techniques for characterization of ancient pottery shards from Conjunto Vilas and São João, located in the Amazonia region. The characterization had the aim of establishing relations between ceramics from the respective sites through identification of similarities and differences observed in the ceramic shards with red and white pigmentation, as well as of engobe and clay paste. To the best of our knowledge, this is the first report on spectroscopic and multivariate studies of the potteries in the Conjunto Vilas and São João sites.

Fig. 1 presents a satellite photograph and the maps of Brazil and the Amazon region; the locations of the Conjunto Vilas and São João sites are indicated near to the Amazon River bank (known in Brazil as the Solimões River). The location coordinates of these sites are: UTM 20M 0313990 9628446/20M 0341007 9611394 (Belletti, 2015; Lopes, 2018).

The samples studied here were from six pottery shards: two of them collected in the São João site (SJ) and four from the Conjunto Vilas (CV). One of the samples from the São João site was of the Tefé phase occupation and the other of the Caiambé phase. Between the four samples from Conjunto Vilas, it was identified a shard of each of the phases (Tefé, Caiambé and Pocó), and another of the Caiambé–Tefé technological flow. The identification of the shards was carried out by archeologists according to the specific characteristics of each piece.

The addition of non-clay (non-plastic) materials, known as tempers, to the raw clay improves its workability, minimizing shrinkage and preventing cracking (Papachristodoulou et al., 2008). The use of organic material can be especially advantageous in cooking vessels, because most of the temper burns out during firing, leaving voids that may interrupt cracks caused by thermal stress during use (Bel, 2015). Examples of tempers widely used in ceramic pastes by these Amazonian cultures are cauxi (a river sponge – sponge spicules) and caraipé (burnt tree bark – siliceous tree-bark ash) (Hazenfratz et al., 2016; Watling et al., 2015; Costa et al., 2010). Fig. 2a and Fig. 2b show examples of these materials. Cauxi is composed of amorphous  $\text{SiO}_2$ . Before being added to the ceramics, caraipé, unlike cauxi, is burned, to obtain only the siliceous base of the material. If this burn is not performed, the presence in the paste of organic material will affect the durability of the ceramic part (Costa et al., 2009).

Potteries of the Caiambé phase have added cauxi as non-plastic material and red engobe as decoration, ceramics with incisions (drawing made with a cutting instrument) and painting also being common. Other characteristic of this phase are motifs with elongated S-shaped, zig-zag, and spirals lines.

Pottery from the Tefé phase has a characteristic use of caraipé as temper and decorative techniques, such as the painting in black and/or red on white engobe, excise and modeling (Belletti, 2015; Hazenfratz et al., 2016). From the Pocó phase, ceramics had added cauxi tempers, with polygonal motifs and polychrome paintings. The pottery of this phase has the peculiarity of being light and porous (Lima and Neves, 2011).

Pigments were used by ancient Amazonian peoples for various purposes, including application of polychromy in ceramics. According to Lopes (2018), for example, the producers of ceramics from the Amazonian polychrome tradition used a characteristic polychrome combination – with red, brown and black colors on a white engobe – to mark their ceramics in an emblematic way.

It is relevant to know about the origin of the previous archeological analyses of ancient ceramics, mainly because this can provide a direction for studies by standard physical analytical techniques, such as Fourier transform infrared (FTIR), X-ray diffraction (XRD), energy-dispersive X-ray fluorescence (ED-XRF), and scanning electron microscopy, coupled with energy-dispersive X-ray spectroscopy (SEM-EDX), that can serve, for example, to identify the types of tempers used in the constitution of archeological pottery, of clay sources, and for comparison between manufacturing techniques (Mangueira et al., 2011; Iordanidis et al., 2009; Papachristodoulou et al., 2008; Seetha and Velraj, 2015). The variation in the chemical composition may imply pottery from different production sites or reflect the natural inhomogeneity of local clay deposits and the application of different manufacturing processes in local workshops (Iordanidis et al., 2009).

## 2. Materials and methods

The pottery shards investigated in this work were collected in the archeological sites Conjunto Vilas and São João, located in the State of Amazonas, more specifically in the city of Tefé, on the margins of the Tefé River and near the Caiambé Lake. The samples were provided by archeologists of the Institute of Sustainable Development Mamirauá

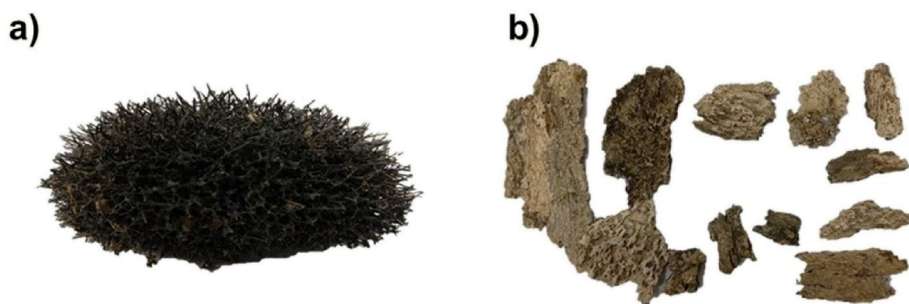


Fig. 2. a) Cauixi (river sponge); b) Fragments of caraipé (siliceous tree bark – burnt tree bark). The material was provided by the archeologist Angislaine Freitas Costa.

(ISDM), through a collaborative project between the Federal University of Sergipe and ISDM. The pottery shards studied were selected according to their macroscopic characteristics, such as pigmentation and type of ceramic paste. From each shard was scraped different samples (pigment, paste and engobe), resulting in a total of ten sub-samples (fragments). The purpose of this partition was to perform detailed analysis of the constituent elements of each fragment.

Of the six pottery shards, fourth were subdivided into paste and pigment. For example, the shard 1 from Conjunto Vilas (CV1), which was composed of paste ceramic (P) covered by a colored (C) pigment layer, was subdivided into two fragments, one composed only of paste (CV1P) and the other of pigment (CV1C). Likewise, one of the samples from the São João site (SJ) was subdivided into two fragments, SJ1P and SJ1C. Table 1 shows the provenance number (PN), the geographical coordinates of each site excavated for sample collection, the depth where each shard was found, and the respective occupation phases. Table 2 shows the techniques used for shard characterization. Spectroscopic techniques were used to analyze the production method, chemical composition, crystalline formations, temperature of burning, elemental characteristics and the presence of non-plastic materials of each shard and type of sub-sample produced. The samples were dried at room temperature and powdered prior to spectroscopic analysis.

As the pigments and pastes analyzed in this work are opaque to visible light, the reflection microscopy technique was chosen to obtain the optical microscopy images of the samples. In this technique, a light focuses on the sample and being reflected and collected by the microscope lens, the superficial details of the sample are highlights. The images were acquired with an Optical Olympus BX-51 microscope equipped with a digital camera LC Color Evolution (PL-A662) with a magnification of up to  $20\times$ , using PixelLink Capture OEM (PixelLink, Ottawa, Canada) image software.

The apparatus used for FTIR was a Varian 640-IR, which has a resolution of  $0.18\text{ cm}^{-1}$ . FTIR spectra were obtained in the range  $4000\text{--}400\text{ cm}^{-1}$ , with 64 scans. Disk-shaped pellets of potassium bromide (KBr) and ceramic powder produced under pressure in a manual press were used in the analyses.

A portable system was used for ED-XRF measurements. The device

Table 1  
Relation of pottery shards and their respective characteristics.

| ID   | Provenance number | Site           | Location       | Depth (cm) | Phase              | Sample        |
|------|-------------------|----------------|----------------|------------|--------------------|---------------|
| CV1C | 911.45            | Conjunto Vilas | S1450E1651     | 50–60      | Technological Flow | White pigment |
| CV1P | 911.45            | Conjunto Vilas | S1450E1651     | 50–60      | Technological Flow | Paste         |
| CV2P | 991.20W           | Conjunto Vilas | S1068E1430     | 80–90      | Pocó               | Paste         |
| CV3C | 987.7             | Conjunto Vilas | S1068E1430     | 60–70      | Caiambé            | Engobe        |
| CV3P | 987.7             | Conjunto Vilas | S1068E1430     | 60–70      | Caiambé            | Paste         |
| CV4C | 993.65            | Conjunto Vilas | S1068E1430 F13 | 80–90      | Tefé               | Red pigment   |
| CV4P | 993.65            | Conjunto Vilas | S1068E1430 F13 | 80–90      | Tefé               | Paste         |
| SJ1C | 804.2B            | São João       | N1196E868      | 20–30      | Tefé               | White pigment |
| SJ1P | 804.2B            | São João       | N1196E868      | 20–30      | Tefé               | Paste         |
| SJ2P | 209.4             | São João       | N1048E1008     | 50–60      | Caiambé            | Paste         |

Table 2  
Imaging and spectroscopy techniques used for characterization of the samples.

| ID   | Optical Microscopy | FTIR | ED-XRF | XRD | SEM-EDX |
|------|--------------------|------|--------|-----|---------|
| CV1C | ✓                  | ✓    | ✓      | ✓   | –       |
| CV1P | ✓                  | ✓    | ✓      | ✓   | –       |
| CV2P | ✓                  | ✓    | ✓      | ✓   | ✓       |
| CV3C | ✓                  | ✓    | ✓      | ✓   | –       |
| CV3P | ✓                  | ✓    | ✓      | ✓   | –       |
| CV4C | ✓                  | ✓    | ✓      | ✓   | –       |
| CV4P | ✓                  | ✓    | ✓      | ✓   | ✓       |
| SJ1C | ✓                  | ✓    | ✓      | ✓   | –       |
| SJ1P | ✓                  | ✓    | ✓      | ✓   | ✓       |
| SJ2P | ✓                  | ✓    | ✓      | ✓   | ✓       |

was a mini X-ray tube with a focal point size of 2 mm, operating with voltages ranging from 10 to 50 kV and currents of 5–200  $\mu\text{A}$  with a silver (Ag) transmission target. The detector used was a Si Drift X-ray semiconductor ( $25\text{ mm}^2 \times 500\text{ }\mu\text{m}$ ) with a thin beryllium end window of  $12.5\text{ }\mu\text{m}$ , and an energy resolution of 125 eV FWHM at 5.9 keV ( $^{55}\text{Fe}$ ). The tube current and voltage used were 20  $\mu\text{A}$  and 30 kV, respectively. The quantification of elemental concentrations was determined by comparison with the reference material “Buffalo River – RM8704” and “Plastic Clay Saracuruna – IPT32” (RM8704, 2018; IPT32, 1980) measured under the same experimental conditions.

The XRD analyses were performed in a Rigako system (ME12773A), which has a  $\text{CuK}\alpha$  wavelength of  $1.54051\text{ }\text{Å}$ , in continuous scan mode at a rate of  $1^\circ$  per minute and with steps of  $0.03^\circ$ . For the analyses, each sample was fixed on a rotating base which performs 15 rotations per minute. The acquisition time for a sample was 3 s in a  $2\theta$  range of  $5\text{--}90^\circ$ . The tube voltage and current used were 40 kV and 30 mA, respectively. To confirm the respective compositions of the samples and their crystalline character, the XRD results were compared with reference patterns obtained from the ICSD database (Inorganic Crystal Structure Database). In order for the program to access the database, a PDF-2 archive (Powder Diffraction File TM) was used, allowing the loading of crystallographic files.

For the SEM analyses a JEOL instrument, model JCM-5700, was

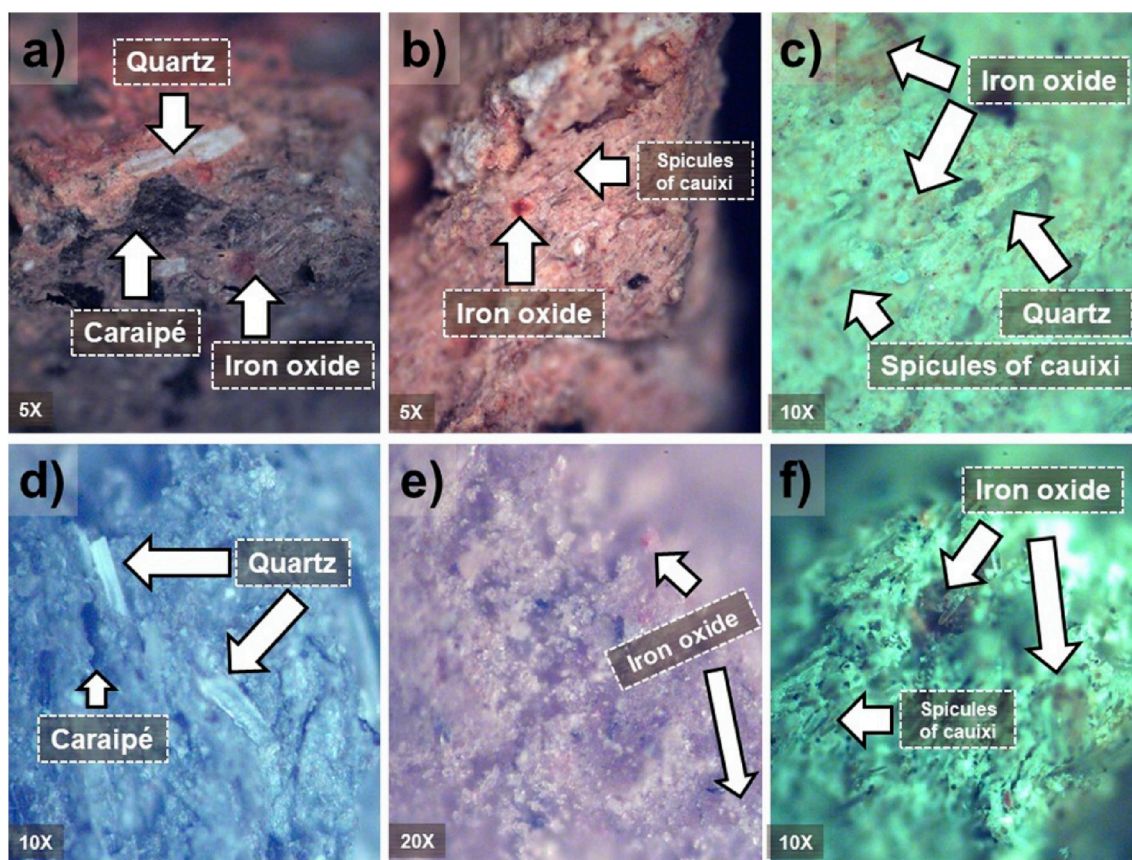


Fig. 3. Optical microscopy images of a) CV4P, b) CV2P, c) CV3P, d) SJ1P, e) SJ2P and f) CV1P ceramic pastes.

used. The device has a minimum resolution of 5 nm, with the acceleration of electrons promoted by a variable voltage of 500 V to 20 kV. In the preparation of the samples, a paste fragment was collected from each pottery shard. Subsequently, the surface of each fragment was sputtered with gold using a metalizer to increase the conductivity of the sample. The SEM images were obtained using a voltage of 10 kV, with magnification from 100 to 10000 $\times$ , ranging from 1 to 100  $\mu\text{m}$ . After an enlarged visualizing of the samples, punctual chemical analyses with SEM-EDX were performed.

### 3. Results and discussion

#### 3.1. Optical microscopy

Optical microscopy measurements enabled initial evaluation of the presence of tempers and minerals in the ceramic pastes. Fig. 3 shows photomicrographs of CV4P, CV2P, CV3P, SJ1P, and SJ2P samples. In the images, the presence of a red pigmentation in CV4P, CV2P, CV3P, and SJ2P samples was observed; this is due to oxidized iron contained in their pastes. It is natural to find oxidized chemical elements in the pastes because the oxidation occurs by natural action of exposure to the humid climate of the region where the archeological sites are located.

In the pigmented samples, the presence of tempers was observed in optical microscopy images. Such observation may be justified considering that CV1C, CV3C, and CV4C ceramic shards have pigmentation as part of the engobe, and the colors are silica-based siliceous base. Fig. 4 shows photomicrographs of CV1C, CV3C, CV4C, and SJ1C shards. The presence of red pigmentation in the CV3C and CV4C samples is evident. These reddish colorations are seen because of the various concentrated oxidation points. The non-plastic materials and quartz are highlighted by arrows in the micrographs.

Fig. 3a shows quartz crystal scattered around the CV4P ceramic

paste, accompanied by caraipe inclusions. Looking more closely, red-colored points can be seen near the inclusion, indicating the presence of oxidized iron in the material. Fig. 3b shows cauxi spicules in CV2P paste and other iron oxidation points. This paste has a different color, indicating large amounts of iron. A clearer coloration was observed in the CV3P paste (Fig. 3c), unlike samples CV4P, CV2P, and SJ2P. It is possible to identify cauxi spicules together with oxidized iron. It was not possible to identify oxidized iron in the SJ1P paste (Fig. 3d); however, temper and quartz crystals were identified in large quantities in this ceramic shard. In Fig. 3e, oxidized iron (red points) were identified, but it was not possible to identify visually the presence of non-plastics in sample SJ2P. In Fig. 3f, cauxi spicules were identified, together with oxidized iron.

The dark spots observed in the CV1P and SJ2P fragments are related to the presence of temper in the ceramics. The dark color indicates carbonization, resulting from the caraipe preparation by burning to eliminate organic residues, in order to maintain just the siliceous base of this temper (Navarro, 2016).

The CV2P and CV3P shards are of pottery from the Pocó and Caiambé phases. In these samples was observed the presence of cauxi spicules protruding from the ceramic paste, as shown by micrography (Fig. 3b). These pastes, which contain cauxi temper, were produced by one of the oldest techniques employed by the Amazonian peoples (Navarro, 2016). The silicon oxide, mainly of quartz structure, is frequently found in the ceramics studied (Hazenfratz et al., 2016). The presence of quartz crystals was identified by optical microscopy of the CV4P, CV2P, CV3P, and SJ1P pastes.

In Fig. 4a we can identify cauxi spicules in the CV1C pigmentation. In this sample, no points of oxidized iron were observed. Fig. 4b shows cauxi spicules and oxidized iron in CV3C. This sample had a different color compared to the other samples, indicating large amounts of iron in the paste. In Fig. 4c quartz crystals are observed in the CV4P,

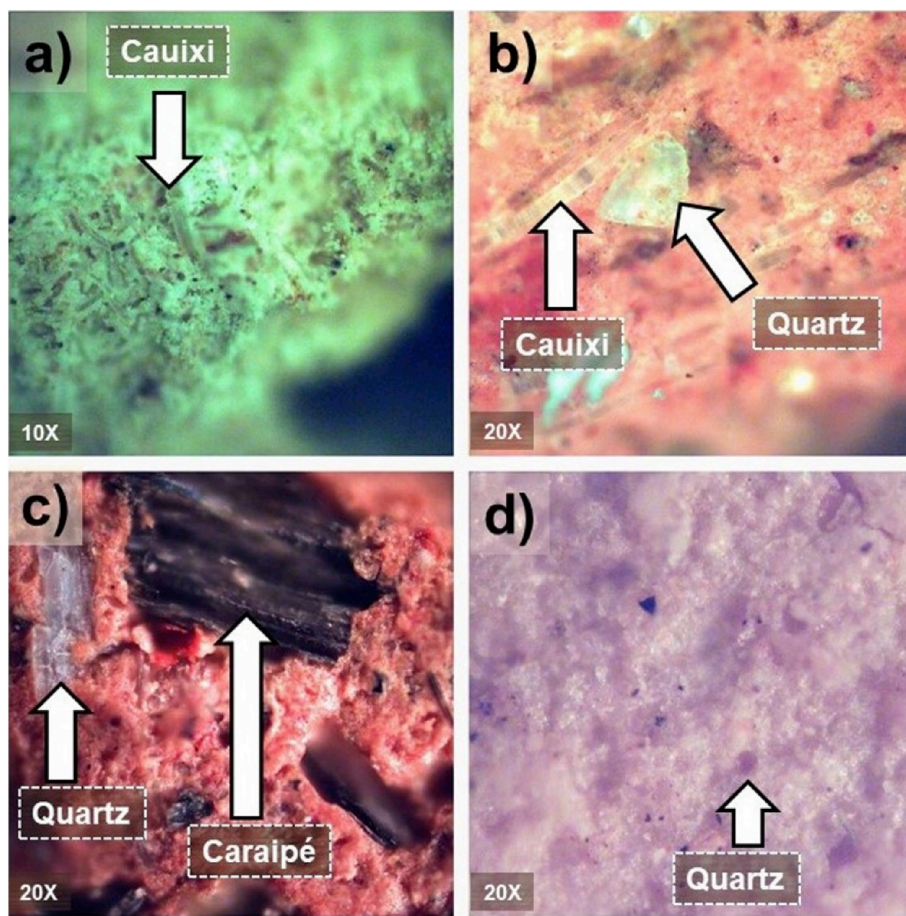


Fig. 4. Optical microscopy images of a) CV1C, b) CV3C, c) CV4C and d) SJ1C ceramic pigments.

accompanied by several black points indicating the presence of caraipé. It was not possible to identify non-plastic or oxidized iron points in SJ1C pigmentation (Fig. 4d) or in its paste (Fig. 3); however, large numbers of quartz crystals were observed in this fragment.

Scanning Electron Microscopy with X-ray Energy Dispersion.

For a comparison between the chemical and structural properties differences of the ceramic pastes, SEM-EDX analyses were performed. Fig. 5 presents photomicrographs of the five pastes (CV2P, CV4P, CV3P, SJ1P and SJ2P). Fig. 6a, b and 6c are uniquely related to the CV4P, CV3P and CV2P pastes. The points marked on these images are focusing points of the SEM-EDX detector. The chemical compositions obtained from these SEM-EDX analyses are presented in Tables 3–5.

Quartz crystals and non-plastics were observed with relative ease in the optical microscopy images. In the results of the SEM-EDX analyses (Tables 3–5), points with high silicon concentrations were also found. However, since SEM-EDX was used as a technique of point chemical analysis, it is justifiable to identify certain chemical elements in small concentrations at different locations in the samples.

The CV4P sample (Fig. 5a) attracted attention due to the different structure observed throughout the ceramic paste. For a more accurate analysis, a closer approximation was made, and a large amount of silicon, oxygen and carbon was evidenced (Table 3). From the photomicrographs shown in Figs. 5a and 6a, considering Table 3, we can suggest the presence of caraipé in the CV4P paste. It is important to emphasize that, again, the punctual character of the SEM-EDX analysis may have hindered the identification of iron in the sample, differently from what was observed in the optical microscopy image of this same sample (Fig. 3a).

In Fig. 5b, structures are shown in dispersed spicule format throughout the CV3P ceramic sample. In Table 4, the SEM-EDX data

shown are from four distinct points where the spicules were observed. In these points, large amounts of silicon were detected. Thus, it is suggested that these spicules originate from the cauixi temper due to its silica-based composition. (Costa et al., 2009; Hazenfratz et al., 2016).

Spicules were also observed in 3-point EDX analysis of the CV2P paste (Fig. 5c). Point 1 presents a large amount of oxygen and silicon, accompanied by aluminum and iron, which are in smaller quantities. In point 2 a great amount of silicon and oxygen can be seen; however, aluminum is in larger quantity if compared to points 1 and 3. At point 3, with elemental quantities similar to point 2, one can see the presence of silicon and oxygen in significant quantities, followed by aluminum and iron.

Large amounts of silicon have been identified by microscopic optical images (Fig. 3b) in the CV3P sample where the spicules are observed. Elsewhere the presence of aluminum has also been identified. From the micrographs and the elemental composition, the presence of cauixi inserted in an aluminosilicate layer is suggested because the analyzed points present a larger amount of silicon and aluminum, as shown in Table 5.

A different structure of cauixi is identified in Fig. 5d. Using a larger magnification factor, one can perceive structures embedded in each other, showing a certain symmetry in SJ2P paste.

Fig. 5e shows the photomicrograph of the SJ2P ceramic shard, in which three clustered crystal structures can be evidenced. In this sample, the predominance of silicon can be seen in these structures, as can a small amount of aluminum. On the outside, the inverse occurs: aluminum is predominant. In this figure, silicon is represented by a red color and the aluminum by green. With these data, it can be suggested that the three structures are quartz crystals wrapped in an aluminosilicate layer.

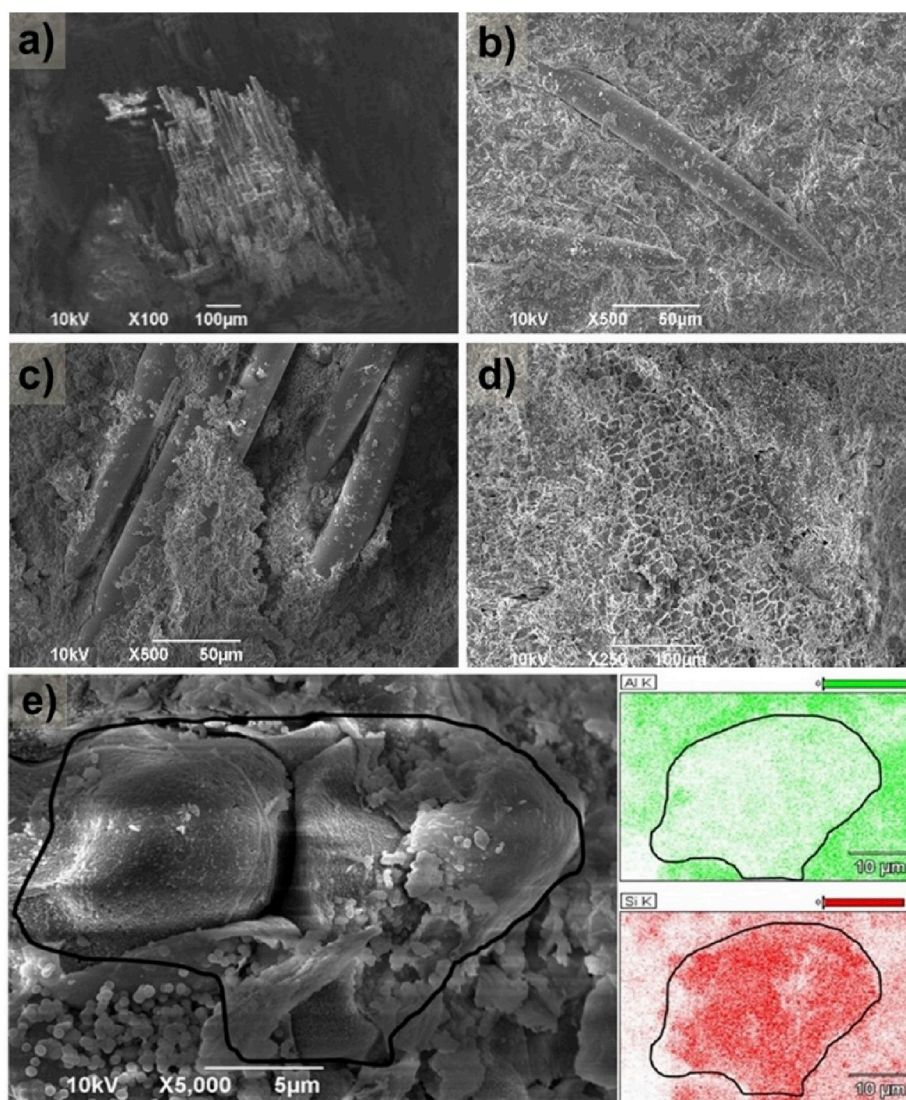


Fig. 5. Scanning electron microscopy of ceramic pastes: a) CV4P b) CV3P c) CV2P d) SJ1P, and e) SJ2P (Si in red and Al in green). (For interpretation of the references to color in this figure legend, the reader is referred to the Web version of this article.)

Comparing Fig. 6d, which shows a photomicrograph of a shell studied by Abreu et al. (2015) as an archeological artifact, with Fig. 5d, we can see a structural similarity between the SJ2P paste and a shell. However, in Fig. 4c, the presence of caraipé temper can be identified, similar to that observed in the CV4P paste (Fig. 3a). With this, it is suggested that shells were used as temper in the preparation of this ceramic, in addition to caraipé.

The SEM-EDX elemental analysis consists of the detection of characteristic X-rays emitted due to the interaction of an electron beam with the sample. The resolution of SEM-EDX images is lower than that obtained by SEM due to the interference of secondary interactions in the sample. The SEM images shown in Fig. 5 served as a reference to identify the quantitative analysis points performed by SEM-EDX (Fig. 6), in order to contribute to the interpretation of the data showed in Tables 3–5

### 3.2. Fourier transform infrared spectroscopy

FTIR analyses were carried out to add information to the elemental characterization of the samples. The results obtained in the range 1600–400  $\text{cm}^{-1}$  were specifically for the inorganic species, as illustrated in Fig. 7. In the FTIR spectra can be seen the doublet bands at 777, 796 and 696  $\text{cm}^{-1}$ , which represent Si–O deformations, identified

as quartz in the figure. Such a result suggests the presence of cauxi and caraipé in the samples, because these tempers contain silicon. Bands in the range of 1000–1100  $\text{cm}^{-1}$  are associated with the stretching of silicon oxide, identified as Si–O–Si. These vibrations may indicate the presence of kaolinite (aluminum silicates) in the ceramic material (Nascimento et al., 2015; Shoval, 2003). Such bands are characteristic of clay minerals and originate from angular deformations of Al–O–Si (Shoval, 2003). The band at 476  $\text{cm}^{-1}$  indicates the presence of iron oxide, which corroborates the amounts of iron detected by microscopic techniques (OM and SEM-EDX), and ED-XRF, as shown in Table 6 and Table 7. The spectra of the pigmented samples are quite similar, as shown in Figs. 7 and 8. Therefore, it is necessary to consider the lower-intensity absorption bands.

### 3.3. Energy dispersive X-ray fluorescence

The concentrations of Si, Fe, Ti, K, Ca, Zn, Sr, Mn, Pb, Rb, Zr, Cu, Cr and Al were identified by ED-XRF analyses. The results showed that Si and Al are the major components in all samples.

Tables 6 and 7 show the elemental composition results from ED-XRF of the ceramic fragments. It is observed that the analyzed clay is comprised predominantly of  $\text{SiO}_2$  and  $\text{Al}_2\text{O}_3$ . These constituents are combined in greater proportion as aluminosilicate. In lower

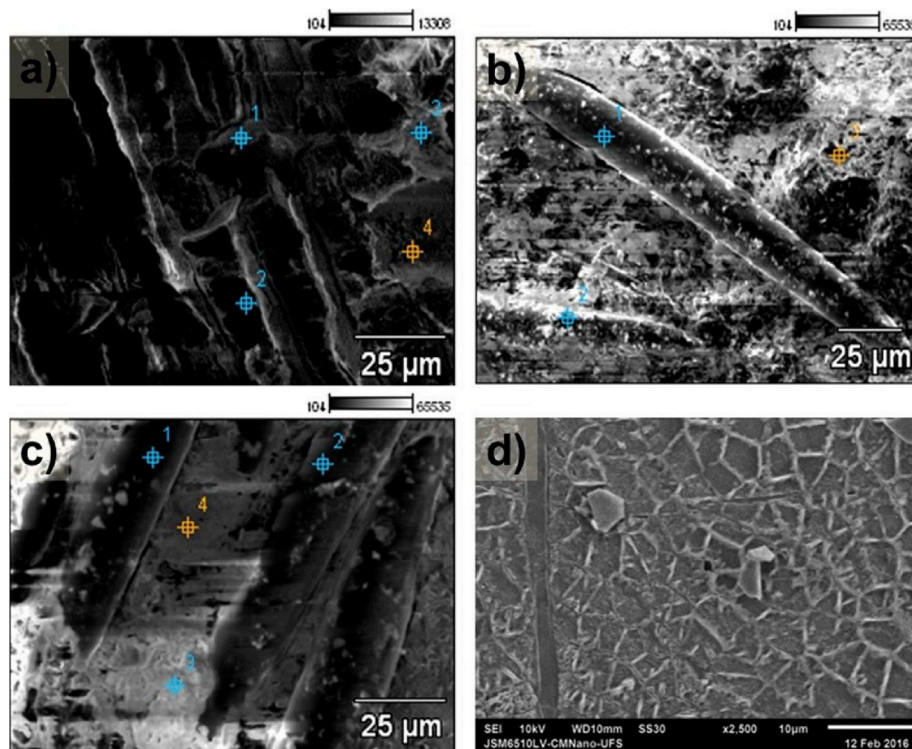


Fig. 6. Scanning electron microscopy in energy-dispersive X-ray analysis mode showing non-plastic materials contained in ceramic pastes (the colored marks indicate the points that were analyzed): a) CV4P, b) CV3P, and c) CV2P. Figure d) shows a photomicrograph of a shell studied by Abreu et al. (2015).

Table 3

Elemental composition obtained by SEM-EDX from the CV4P paste measured at the points identified in Fig. 6.

| Point | C     | O     | Al   | Si    | P    | Cl   | Ca   |
|-------|-------|-------|------|-------|------|------|------|
| 1     | 5.85  | 46.49 | 0.65 | 45.03 | –    | 1.98 | –    |
| 2     | 15.77 | 28.03 | 1.83 | 53.05 | 1.32 | –    | –    |
| 3     | 4.91  | 30.69 | 9.70 | 44.53 | 5.66 | 2.50 | 2.01 |
| 4     | 8.65  | 15.95 | 7.27 | 56.97 | 3.62 | 3.45 | 4.09 |

Table 4

Elemental composition obtained by SEM-EDX from the CV3P paste measured at the points identified in Fig. 6.

| Point | C    | O     | Mg   | Al    | Si    | P    | Fe   |
|-------|------|-------|------|-------|-------|------|------|
| 1     | 2.82 | 45.39 | –    | 9.66  | 32.52 | 1.20 | 8.42 |
| 2     | 8.54 | 45.02 | –    | 16.21 | 25.36 | 4.87 | –    |
| 3     | 1.22 | 50.92 | 0.23 | 8.82  | 30.66 | 1.92 | 6.20 |

Table 5

Elemental composition obtained by SEM-EDX from the CV2P paste measured at the points identified in Fig. 6.

| Point | C     | O     | Mg   | Al    | Si    | P     | Cl   | K    | Ca   | Fe   |
|-------|-------|-------|------|-------|-------|-------|------|------|------|------|
| 1     | 6.03  | 35.50 | 0.15 | 0.60  | 54.21 | 0.33  | 3.18 | –    | –    | –    |
| 2     | 10.93 | 11.87 | –    | 1.30  | 75.46 | 0.45  | –    | –    | –    | –    |
| 3     | 2.04  | 27.93 | –    | 18.86 | 8.05  | 25.55 | –    | 1.32 | 9.43 | 6.82 |
| 4     | 2.41  | 25.98 | –    | 18.41 | 17.59 | 20.11 | 4.05 | –    | 6.41 | 5.04 |

percentages are the oxides  $K_2O$ ,  $CaO$ ,  $TiO_2$  and  $Fe_2O_3$ , which are present in the chemical composition of the soil of the Amazon region (Costa et al., 2004; Costa et al., 2010; Menezes et al., 2013; Munita and Carvalho, 2015).

It is observed that  $SiO_2$  and  $Al_2O_3$  are predominant in the analyzed clay, and these compounds are practically in the same proportion as the

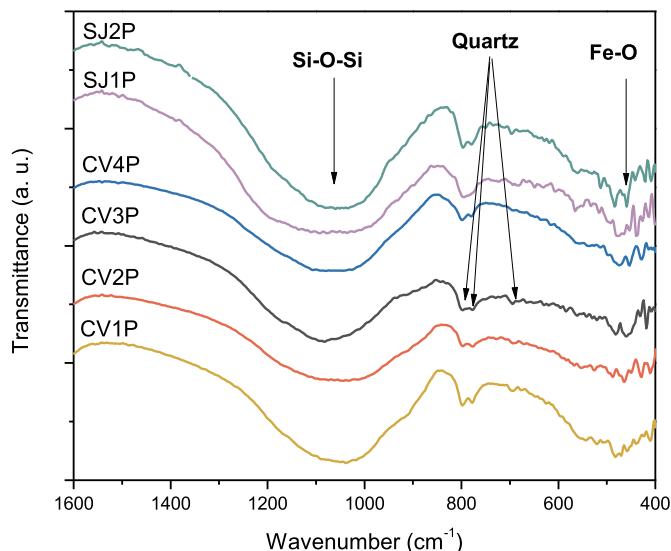


Fig. 7. FTIR spectra of ceramic pastes from Conjunto Vilas and São João.

ceramic pastes shown in Table 6.  $K_2O$ ,  $CaO$ ,  $TiO_2$  and  $Fe_2O_3$ , which are the elements responsible for pigmentation, appear in small percentages. The CV4C and CV3C ceramic shards, with red pigmentation, have a higher percentage of iron than do the CV1C and SJ1C ceramics with white pigmentation.

The data obtained with the ED-XRF technique allowed for a broader understanding of the elemental compositions of the samples, since it is a quantitative and qualitative technique that analyzes a sample in its entirety, not only in a punctual or superficial way.

Dispersion graphs were organized from the results obtained from ED-XRF. This was carried out with the aim of identifying similarities and differences between the raw materials used in the production of the pottery shards studied, through correlation between the chemical

**Table 6**  
Chemical analysis (ED-XRF) of pottery shards (pastes) from Conjunto Vilas and São João sites.

| ID           | Al <sub>2</sub> O <sub>3</sub> (%) | SiO <sub>2</sub> (%) | K <sub>2</sub> O (%) | CaO (%)   | TiO <sub>2</sub> (%) | Fe <sub>2</sub> O <sub>3</sub> (%) |
|--------------|------------------------------------|----------------------|----------------------|-----------|----------------------|------------------------------------|
| CV1P Tefé    | 20 ± 2                             | 60 ± 3               | 1.1 ± 0.1            | 1.0 ± 0.1 | 0.8 ± 0.04           | 3.5 ± 0.2                          |
| CV4P Tefé    | 15 ± 2                             | 65 ± 3               | 0.8 ± 0.1            | 1.1 ± 0.2 | 0.73 ± 0.03          | 4.1 ± 0.2                          |
| CV3P Caiambé | 25 ± 3                             | 53 ± 3               | 0.7 ± 0.1            | 0.7 ± 0.1 | 1.16 ± 0.05          | 5.7 ± 0.3                          |
| CV2P Pocó    | 19 ± 2                             | 58 ± 3               | 1.5 ± 0.1            | 1.5 ± 0.2 | 1.08 ± 0.05          | 4.9 ± 0.2                          |
| SJ2P Caiambé | 22 ± 3                             | 58 ± 3               | 1.3 ± 0.1            | 0.6 ± 0.1 | 0.96 ± 0.04          | 3.3 ± 0.1                          |
| SJ1P Tefé    | 20 ± 2                             | 60 ± 3               | 1.3 ± 0.1            | 0.7 ± 0.1 | 1.1 ± 0.05           | 3.1 ± 0.1                          |

elements identified. Minority elements, such as Mn, Zn, Sr, Zr, found in the samples were important to perform the group separations. A similar behavior of group separation was illustrated in the work of Munita et al. (2005). These authors studied the chemical and mineral composition of ceramics from the Asurini village (Asurini do Xingu, Brazil) trying to understand the criteria in the selection of raw materials by means of instrumental neutron activation analysis and scanning electron microscopy.

The groupings in the dispersion graphs (areas of the peaks that identify the chemical elements in each sample) make it possible to verify how the samples are related, showing their similarities or differences according to their data. It can be seen from the graphs shown in Fig. 9 that there are some differences between the elemental quantities of Mn and Zn (Fig. 9a), Zn and Fe (Fig. 9b), Sr and Al (Fig. 9c), and Zr and Ca (Fig. 9d) in the samples from the Conjunto Vilas and São João sites. In the graphs, the red points, corresponding to the São João site, are in different regions than the blue points related to samples from Conjunto Vilas. With this, it is suggested that the ceramics from the Conjunto Vilas site were produced from different raw materials from those from São João; that is, the sources of clays and tempers are not the same.

### 3.4. X-ray diffractometry

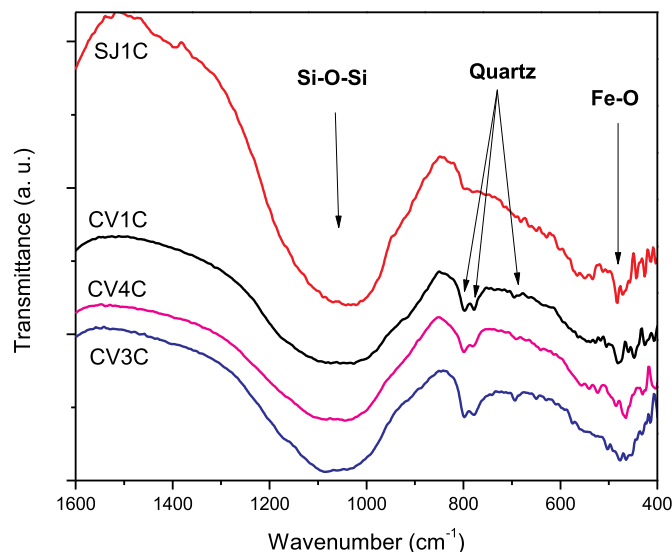
The predominant crystalline phases identified in the XRD spectra of the studied sites are quartz, hematite, kaolinite, anatase, dolomite and illite-muscovite. Kaolinite was most frequently found in the spectra of sediment impregnated in the ceramics, indicating that the ceramic pastes were fired cooked at a temperature higher than 650 °C (Martirena et al., 2018).

Fig. 10 shows X-ray diffractograms of the CV4P, CV2P, CV3P, SJ1P, SJ2P ceramic pastes. The identified crystallographic phases are reported in Table 8. Quartz is observed to be the major component in the typical raw clay from the sites covered in this study. The presence of iron oxide is suggested due to the identification of hematite peaks. The XRD spectra of these ceramic pastes indicate a very similar mineralogical composition. Table 8 also presents the crystallographic data sheet (PDF-2) of each crystalline phase.

In Fig. 11, quartz is also confirmed as the major component. This clay is characteristic of the ceramics and, consequently, of the artifacts from the sites covered in this study. The spectra of the red pigmentation of samples CV4C and CV3C show peaks characteristic of iron oxide accompanied by illite peaks similar to CV1C and SJ1C samples. In the analysis, the fact that the hematite peak does not appear in its spectra is striking. The other phases correspond to the phases of the crystallographic charts described in Table 8.

**Table 7**  
Chemical analysis (ED-XRF) of pigments of pottery shards from Conjunto Vilas and São João sites.

| ID           | Al <sub>2</sub> O <sub>3</sub> (%) | SiO <sub>2</sub> (%) | K <sub>2</sub> O (%) | CaO (%)   | TiO <sub>2</sub> (%) | Fe <sub>2</sub> O <sub>3</sub> (%) |
|--------------|------------------------------------|----------------------|----------------------|-----------|----------------------|------------------------------------|
| CV1C (white) | 22 ± 3                             | 58 ± 3               | 1.2 ± 0.1            | 1.0 ± 0.1 | 0.83 ± 0.04          | 4.0 ± 0.2                          |
| SJ1C (white) | 25 ± 3                             | 53 ± 3               | 1.9 ± 0.1            | 0.5 ± 0.1 | 2.1 ± 0.09           | 3.8 ± 0.2                          |
| CV4C (red)   | 15 ± 2                             | 65 ± 3               | 0.6 ± 0.1            | 0.9 ± 0.1 | 0.60 ± 0.03          | 3.3 ± 0.1                          |
| CV3C (red)   | 18 ± 2                             | 59 ± 3               | 1.3 ± 0.1            | 0.7 ± 0.1 | 1.18 ± 0.05          | 6.0 ± 0.3                          |



**Fig. 8.** FTIR spectra of pigmentate samples of the Conjunto Vilas and São João.

Oxidized iron can be obtained with thermal energy uptake by lepidocrocite ( $\gamma$ -FeO.OH), which is a crystalline phase having a metastable cubic structure. After heating, the lepidocrocite adopts a rhombohedral structure and, depending on the mineral connections present in the ceramics, maghemite (250 °C), and goethite or hematite (450 °C) appears with exposure for 2 h to organic material (Cornell and Schwertmann, 2003). The identification of this band around 470 cm<sup>-1</sup> in the FTIR spectra corroborates the high iron contents identified by ED-XRF.

## 4. Conclusions

The archeometric study of the archeological pottery shards from the Conjunto Vilas and São João sites, located in the region of the middle Solimões River, in the central region of Amazonas, enabled us to understand some of the technological aspects related to the raw materials and processes used in the production of the ancient pottery investigated.

As expected, the ED-XRF data showed a large quantity of SiO<sub>2</sub> and Al<sub>2</sub>O<sub>3</sub>, since the ceramic shards have aluminosilicate in raw clay and silicon-based non-plastic materials as their main constituents. By grouping the results obtained in ED-XRF analyses, it was possible to perceive certain differences between the elemental compositions of

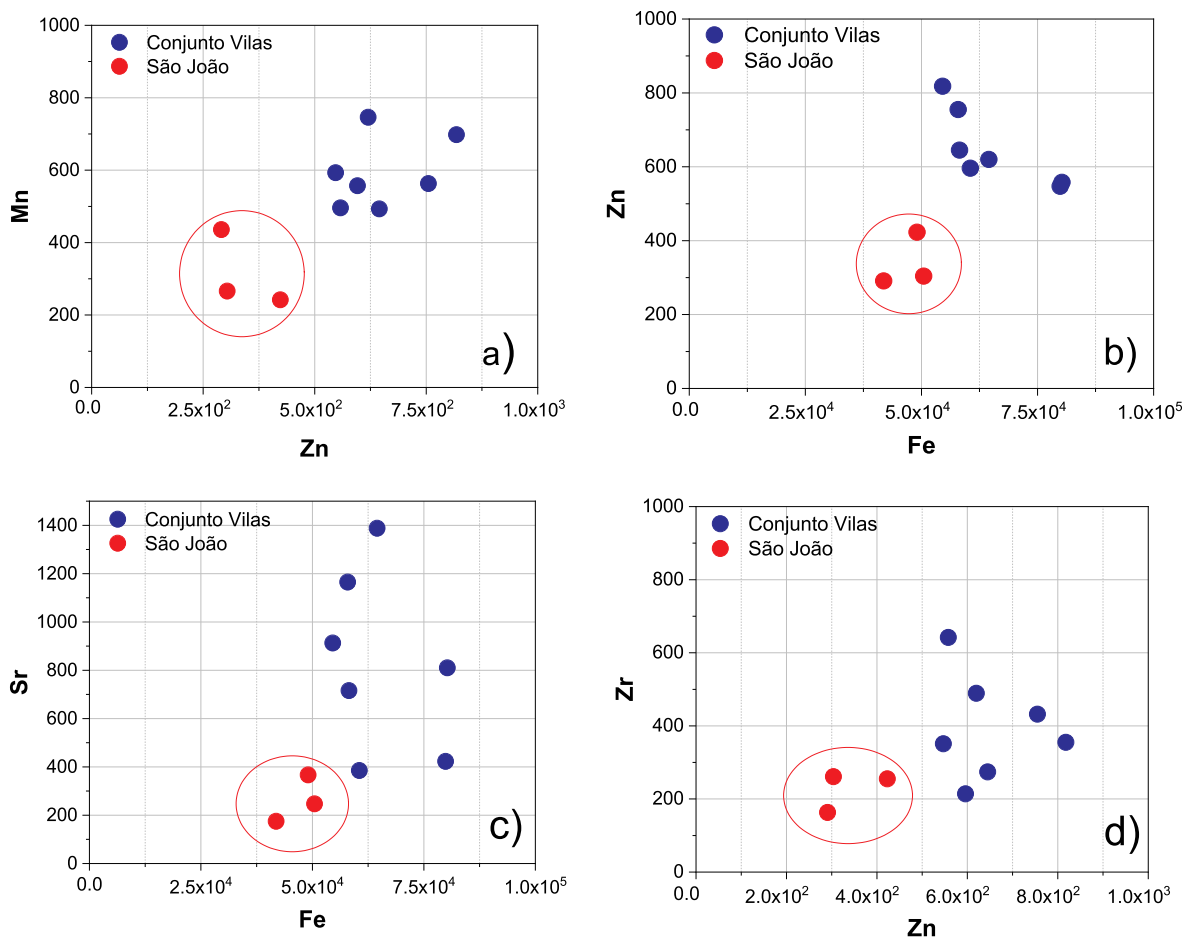


Fig. 9. Dispersion graphs, organized from the results obtained by ED-XRF, showing differences between the elemental quantities in the samples from the Conjunto Vilas and São João sites: a) manganese (y-axis), zinc (x-axis); b) zinc (y-axis), iron (x-axis); c) strontium (y-axis), aluminum (x-axis); d) zirconium (y-axis), calcium (x-axis).

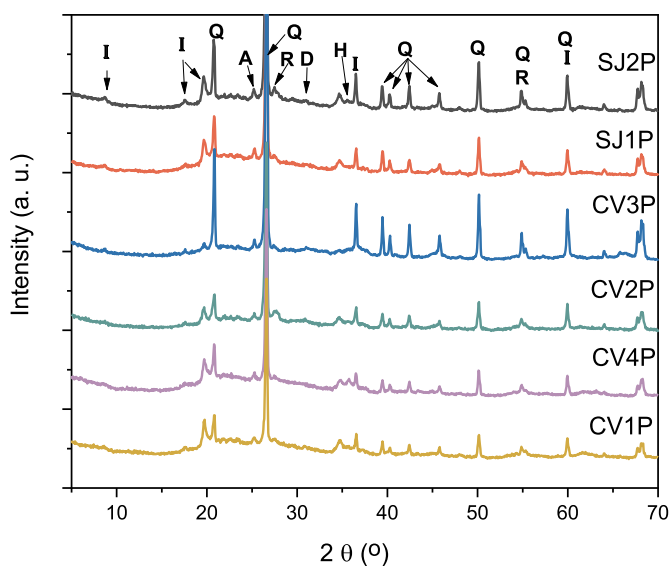


Fig. 10. XRD spectra of ceramic pastes from Conjunto Vilas and São João sites. The peaks are identified as quartz (Q), anatase (A), rutile (R), dolomite (D), hematite (H), and illite-muscovite (I).

samples from each site. With this it can be suggested that the clay sources used in the preparation of the pottery from Conjunto Vilas and São João sites are different. Mn, Zn, Sr and Ca are the chemical

Table 8

Crystalline phases compatible with the XRD spectra of samples from Conjunto Vilas and São João sites.

| Crystalline phase | Chemical Formula  | PDF-2       |
|-------------------|---|-------------|
| Quartz            | SiO <sub>2</sub>  | 00-046-1045 |
| Hematite          | FeO <sub>3</sub>  | 00-033-0664 |
| Kaolinite         | Al <sub>2</sub> Si <sub>2</sub> O <sub>5</sub> (OH) <sub>4</sub>                          | 00-001-0527 |
| Anatase           | TiO <sub>2</sub>  | 00-021-1272 |
| Rutile            | TiO <sub>2</sub>  | 00-021-1276 |
| Dolomite          | CaMg(CO <sub>3</sub> ) <sub>2</sub>   | 00-011-0078 |
| Muscovite         | H <sub>2</sub> KAl <sub>3</sub> (SiO <sub>4</sub> ) <sub>3</sub>                          | 00-001-1098 |
| Illite            | KAl <sub>4</sub> (SiAl) <sub>6</sub> O <sub>20</sub> (OH) <sub>4</sub> + H <sub>2</sub> O | 00-007-0330 |

elements that contributed to highlight the distinction between the clay sources. This result reaffirms that the characterization of the chemical composition of ceramic artifacts subsidizes the identification of the chosen sources of raw material employed in the manufacturing of the archeological ceramics. Such an idea agrees with work of Munita et al. (2005) on the collection sites for raw materials used to produce ancient indigenous ceramics in Brazil.

The use of optical microscopy and SEM images, associated with quantitative and semi-quantitative chemical data, enabled the identification of cauxi and caraipé tempers in the pastes, and of Al, Si, K Ca, Ti and Fe and some other minor elements. However, this correlation was not always possible, because SEM-EDX was used as an analytical method for point chemical analysis. Therefore, this justifies the identification of certain chemical elements that were not observed in other

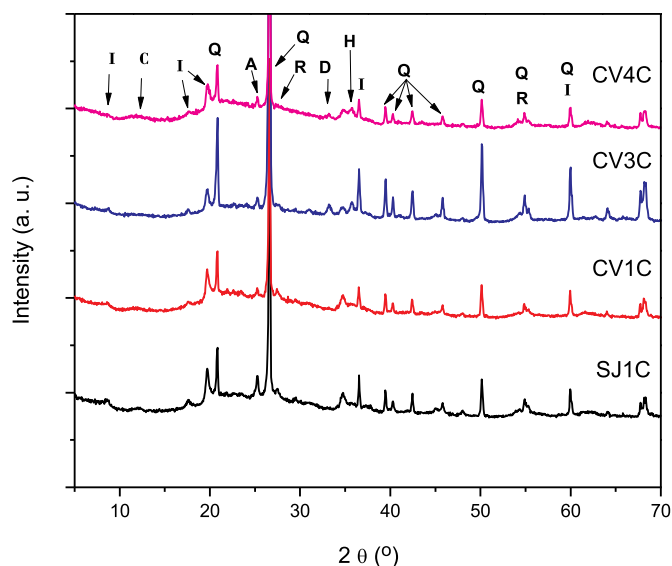


Fig. 11. XRD spectra of ceramic pigmentation from Conjunto Vilas and São João sites. The peaks are identified as quartz (Q), kaolinite (C), anatase (A), rutile (R), dolomite (D), hematite (H), and illite-muscovite (I).

microscopic analyzes. Likewise, it is possible that some elements observed by SEM-EDX have not been identified by the other techniques.

The crystalline phases identified by diffraction were quartz, hematite, kaolinite, anatase, dolomite and illite-muscovite. Kaolinite was the most frequently found, related to the sediment impregnated in the ceramics. Significant changes in the spectra have been identified and red and white pigmentations can be differentiated through the hematite and anatase phases.

These results indicate that archeometric analysis can assertively contribute to elucidation of archeological issues related to the production technology (temperature and composition of pigments) and inter-site issues (provenance of raw materials). However, as noted here, it is necessary to increase the number of samples from ancient potteries to obtain broader conclusions that may answer archeological questions.

## Acknowledgments

This study was financed in part by the Coordenação de Aperfeiçoamento de Pessoal de Nível Superior - Brasil (CAPES) - Finance Code 23038.007416/2012-79 and Conselho Nacional de Desenvolvimento Científico e Tecnológico - Brazil (CNPq) - Finance Code 308090/20160.

## References

- Abreu, C.M., Lima, F.B., Guimaraes, C.R.P., Souza, D.N., Queiroz, A.N., 2015. Análise de Conchas arqueológicas em Sergipe - Alagoas, Brasil. In: XI Congresso Ibérico de Arqueometria, 2015, Évora, Portugal: 1: 5 (In Portuguese).
- Artoli, G., 2010. Scientific Methods and Cultural Heritage. Oxford University Press.
- Bel, M. M. van den, 2015. Archeological Investigations between Cayenne Island and the Maroni River: A Cultural Sequence of Western Coastal French Guiana from 5000 BP

- to Present. Sidestone Press, Leiden.
- Belletti, J.D.S., 2015. Arqueologia do Lago Tefé e a expansão policroma. 2015. 433 f. Dissertação (Mestrado em Arqueologia) - Museu de Arqueologia e Etnologia, Universidade de São Paulo, São Paulo (In Portuguese).
- Cornell, R.M., Schwertmann, U., 2003. The Iron Oxides: Structure, Properties, Reactions, Occurrences and Uses, 2 Ed. John Wiley & Sons, New Jersey.
- Costa, M.L., Carmo, M.S., Oliveira, E., Lima, H.N., Kern, D.C., Goeske, J.A., 2010. Mineralogia e composição química de fragmentos de cerâmicas arqueológicas em sítios de terra Preta de Índio. In: In: Teixeira, W., Madari, B., Mentos, V., Kern, D., Falcao, N., Org (Eds.), As Terras Pretas de Índio da Amazônia: Sua Caracterização e Uso deste Conhecimento na Criação de Novas Áreas. 1ed. Manaus, vol. 1. Embrapa Amazônia Ocidental, pp. 225–241 (In Portuguese).
- Costa, M.L., Kern, D.C., Pinto, A.H.E., Souza, J.R.T., 2004. The ceramic artifacts in archeological black earth (terra preta) from Lower Amazon Region, Brazil: chemistry and geochemical evolution. Acta Amazonica 34, 375–386 (In Portuguese).
- Garcia, L., Costa, J.A., Kern, D.C., Frazão, F.J.L., 2015. Caracterização de solos com terra preta: estudo de caso em um sítio tupi-guarani pré-colonial da Amazônia oriental. Rev. Arqueol. 28, 52–81 (In Portuguese).
- Hazenfratz, R., Munita, C.S., Glascock, M.D., Glascock, E.G.N., 2016. Study of exchange networks between two Amazon archeological sites by INAA. J. Radioanal. Nucl. Chem. 309, 195–205.
- Hilbert, K., 2009. Uma biografia de Peter Paul Hilbert: a história de quem partiu para ver a Amazônia. Boletim do Museu Paraense Emílio Goeldi Ciências Humanas 4, 134–154 (In Portuguese).
- Hilbert, P., Hilbert, K., 1980. Resultados preliminares da pesquisa arqueológica nos rios Nhamunda e Trombetas, Baixo Amazonas, Boletim do Museu Paraense Emílio Goeldi. Nova Série 75, 1–15 (In Portuguese).
- Iordanidis, A., Garcia-Guinea, J., Karamitrou-Mentessidi, G., 2009. Analytical study of ancient pottery from the archeological site of Aiani, northern Greece. Mater. Char. 60, 292–302.
- IPT32, 1980. Padrão Laboratorial Referência 32. Instituto de Pesquisas tecnológicas do Estado de São Paulo, São Paulo. [http://www.ipt.br/materiais\\_ref.php?m\\_tp=2&mf=24&familia=24](http://www.ipt.br/materiais_ref.php?m_tp=2&mf=24&familia=24) accessed Mar/2018.
- Lima, H.P., Neves, E.G., 2011. Cerâmicas da Tradição Borda Incisa/Barrancóide na Amazônia Central. Revista do Museu de Arqueologia e Etnologia 21, 205–230 (In Portuguese).
- Lopes, R.C.D.A., 2018. A tradição policroma da Amazônia no contexto do Médio Rio Solimões (AM) Dissertação (Mestrado em Arqueologia). Universidade Federal de Sergipe (In Portuguese).
- Mangueira, G.M., Toledo, R., Teixeira, S., Franco, R.W.A., 2011. A study of the firing temperature of archeological pottery by X-ray diffraction and electron paramagnetic resonance. J. Phys. Chem. Solids 72, 90–96.
- Martirena, F., Favier, A., Scrivener, C., 2018. Calcined Clays for Sustainable Concret. Springer.
- Menezes, J.A., Souza, W.B., Santana, G.P., 2013. Caracterização de óxidos de ferro presentes em fragmentos cerâmicos de Terra Preta de Índio. Scientia Amazonia 2, 4–10 (In Portuguese).
- Munita, C.S., Carvalho, P.R., 2015. Grupo de Estudos arqueométricos do IPEN-CNEN/SP. Revista Cadernos do Geom 28, 53–59 (In Portuguese).
- Munita, C., Silva, M.A., Silva, F., Oliveira, P., 2005. Archeometric study of clay deposits from the indigenous land of the Asurini do Xingu. Instrum. Sci. Technol. 33, 161–173.
- Nascimento, M.R., Diniz, A.M.P., De Oliveira Araújo, M.H.P., 2015. Reaproveitamento do rejeito de caulim, de Junco do Seridó-PB, na síntese de zeólitas. Revista Principia 23, 77–86 (In Portuguese).
- Navarro, A.G., 2016. Art and style on the Brazilian pile dwellings. Arquivos do Museu de História Natural e Jardim Botânico 25, 100–124.
- Papachristodoulou, C., Oikonomou, A., Ioannides, K., Gravani, K., 2008. A study of ancient pottery by means of X-ray fluorescence spectroscopy, multivariate statistics and mineralogical analysis. Anal. Chem. Acta 573–574, 347–353.
- RM8704 Padrão de sedimento "Buffalo River. <https://www.s.nist.gov/srmors/certificates/8704.pdf> access in mar/2018.
- Seetha, D., Velraj, G., 2015. Spectroscopic and statistical approach of archeological artifacts recently excavated from Tamilnadu, South India. Spectrochim. Acta Mol. Biomol. Spectrosc. 149, 59–68.
- Shoval, S., 2003. Using FT-IR spectroscopy for study of calcareous ancient ceramics. Opt. Mater. 24, 117–122.
- Silverman, H., 2008. The Handbook of South American Archeology. Springer.
- Watling, J., Saunaluoma, S., Pärssinen, M., Schaan, D., 2015. Subsistence practices among earthwork builders: phytolith evidence from archeological sites in the southwest Amazonian interfluvies. J. Archeol. Sci.: Rep. 4, 541–551.